Energetic charged particles in the terrestrial magnetosphere: Cluster/RAPID results

Elena A. Kronberg[1], Patrick W. Daly[2], Elena E. Grigorenko[3], Artem Smirnov[4], Berndt Klecker[5], and Andrey Yu. Malykhin[3]

[1]Ludwig Maximilian University of Munich
[2]Max-Planck Institut fuer Sonnensystemforschung
[3]Space Research Institute of RAS
[4]Helmholtz Centre Potsdam GFZ German Research Centre for Geosciences
[5]MPI

November 26, 2022

Abstract

Energetic charged particles ˜>40 keV can affect the plasma temperature and pressure and as a consequence the whole dynamics of the magnetosphere. How do particles get to such energies is a fundamental science question. Energetic particles are also potentially hazardous for the space observations. It is, therefore, necessary to study the origin of energetic plasma, its acceleration, distribution and consequences on the magnetospheric dynamics. In this work we review the related results based on observations from the Cluster/RAPID energetic charged particle detector. These results represent new insights in plasma acceleration, unexpected features in its distributions, effects on substorm and geomagnetic storm dynamics and remediated observations in the radiation belts during approximately 1.5 solar cycles.

Energetic charged particles in the terrestrial magnetosphere: Cluster/RAPID results

E. A. Kronberg[1], P. W. Daly[2], E. E. Grigorenko[3,4], A. G. Smirnov[5,6,7], B. Klecker[8] and A. Yu. Malykhin[3]

[1]Department of Earth and Environmental Sciences, Ludwig Maximilian University of Munich, Munich, Germany.
[2]Max Planck Institute for Solar System Research, Göttingen, Germany.
[3]Space Research Institute, Russian Academy of Sciences, Russia.
[4]Moscow Institute of Physics and Technology, Moscow, Russia.
[5]Helmholtz-Centre Potsdam - GFZ German Research Centre for Geosciences, Potsdam, Germany.
[6]Institute of Physics and Astronomy, University of Potsdam, Potsdam, Germany.
[7]Geophysical Center of the Russian Academy of Sciences, Moscow, Russia.
[8]Max Planck Institute for Extraterrestrial physics, Garching, Germany.

Key Points:

- Energetic particles at energies >40 keV have to be considered for the plasma temperature and pressure calculations
- Effective acceleration is due to interaction of charged particles with multi-scale magnetic structures and/or electromagnetic fluctuations
- Direction of Interplanetary Magnetic Field leads to ion distribution asymmetries between Northern and Southern hemispheres

Corresponding author: Elena Kronberg, `kronberg@geophysik.uni-muenchen.de`

Abstract
Energetic charged particles ∼>40 keV can affect the plasma temperature and pressure and as a consequence the whole dynamics of the magnetosphere. How do particles get to such energies is a fundamental science question. Energetic particles are also potentially hazardous for the space observations. It is, therefore, necessary to study the origin of energetic plasma, its acceleration, distribution and consequences on the magnetospheric dynamics. In this work we review the related results based on observations from the Cluster/RAPID energetic charged particle detector. These results represent new insights in plasma acceleration, unexpected features in its distributions, effects on substorm and geomagnetic storm dynamics and remediated observations in the radiation belts during approximately 1.5 solar cycles.

Plain Language Summary

Acceleration of plasma in the universe is a fundamental science question. Understanding of acceleration at supernovae shocks, of cosmic jets or laboratory plasmas still has many open questions. Near-Earth space environment is an excellent laboratory to investigate plasma dynamics and to reveal fundamental laws it obeys. Energetic plasmas are also hazardous for space satellites and play a key role in space weather. It is, therefore, necessary to study the energization of space plasmas, their distribution and consequences on the magnetospheric dynamics. In situ observations in the near-Earth space by Cluster satellites and energetic particle detector, RAPID, reveal new insights in plasma acceleration, unexpected features in its distributions and effects on substorm and geomagnetic storm dynamics. These observations also help space weather applications to determine the level of energetic particle intensities.

1 Introduction

The terrestrial magnetosphere is an effective plasma accelerator. There are two main sources for the magnetospheric plasma: the solar wind and the ionosphere.

The solar wind ion population consists mainly of protons. The abundance of He^{++} is in the range of 3% to 6% with variations observed at times of up to 30% (Neugebauer, 1981; Aellig et al., 2001; Kasper et al., 2007; Borrini et al., 1982). The abundance of other heavy ions is <0.1% (including O^{6+}) (Gloeckler & Geiss, 1989). The number of solar wind electrons maintains the charge neutrality in the plasma media. The energy of the pristine solar wind at ∼1 Astronomical Unit is about 1 keV with a Maxwellian core and steeply falling power law part of the spectral distribution for protons (see Figure 1) and about 10s of eV for the electrons which have harder distribution at higher energies than protons. The solar wind interacts with the magnetic field of the Earth, forms the bow shock and then enters in to the magnetosphere via magnetic reconnection and Kelvin-Helmholtz instability. However, in the upstream region of the Earth's bow shock and in the plasma sheet region we observe strong hardening of the power law part of the proton spectrum compared to those in the solar wind, see Figure 1. This implies strong proton energization. Also electrons are strongly energized in the plasma sheet.

The ionosphere delivers to the magnetosphere protons, He^+, N^+, O^+, and the molecular ions NO^+ and O_2^+ (Yau et al., 1991). The dominant heavy ion is O^+ and it is considered as a main tracer of the ions of the ionospheric origin. Electrons flow out from the ionosphere to keep overall the charge neutrality. However, their plasma characteristics are not well studied yet (Borovsky et al., 2020). The ionospheric charged particles outflow on the open and closed magnetic field lines into the magnetosphere. The temperature of the outflowing ionospheric ions in the lobes is about 7 eV (Kronberg et al., 2014). The observed temperature in the plasma sheet is about 20 keV (Malykhin et al., 2020). This means that the oxygen ions are strongly energized in the plasma sheet.

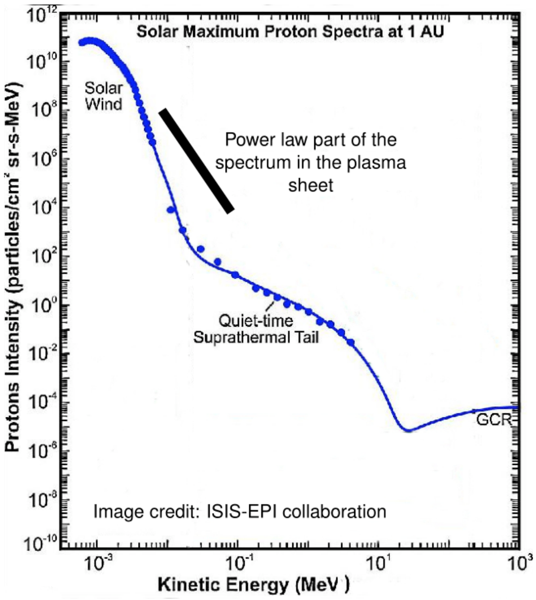

Figure 1. The proton spectra in the solar wind measured by the Parker Solar Probe is indicated by the blue line. The slope of the black bar is equivalent to the spectral slope in the plasma sheet during quiet time taken from Kronberg et al. (2010). Adapted from McComas et al. (2016).

Energized particles play an important role in the dynamics of the terrestrial magnetosphere. Here under energetic we mean electrons in the range from 40 to 400 keV and ions from ∼30 keV to 4 MeV. These energy ranges are determined by the capabilities of the energetic particle detector RAPID on the Cluster mission. Such energetic particles can affect the plasma temperature and pressure and as a consequence the whole dynamics of the magnetosphere starting from small scales such as wave properties and plasma instabilities towards the large scale dynamics of the magnetic storms and substorms.

Another crucial aspect is the effects of such energetic particles on space observations and space weather. Electrons and protons at these energies can lead, for example, to spacecraft anomalies related to surface charging (Matéo-Vélez et al., 2018). The protons at energies of ∼100 keV can enter inside X-Ray telescopes and produce erroneous signal leading to loss of astrophysical and cosmological observations (Fioretti et al., 2016).

It is, therefore, necessary to study the origin of energetic plasma which is mainly related to investigation of acceleration mechanisms leading to the observed spectra hardening, distribution of energetic plasma and consequences of its presence on the magnetospheric dynamics.

In this work we present the related results from the observations by the Cluster/RAPID instrument which is described in Section 2. We discuss the origin of the energetic particles in the region upstream of the bow shock during solar maximum and declining phase of a solar cycle in Section 3. The acceleration of charged particles in the plasma sheet is considered in Section 4. We discuss the distribution of the energized ions on closed magnetic field lines beyond the radiation belts in Section 5. Features of substorm dynamics revealed using energetic particle observations are shown in Section 6. Influence of energetic ions on the dynamics of the magnetic storms is demonstrated in Section 7. Caveats in measurements of the radiation belts and their dynamics are discussed in Section 8. A summary of this review can be found in Section 9.

2 Instrumentation and methods

The Cluster mission consists of 4 identical satellites launched July-August 2000 into a highly elliptical polar orbit (initially 4 × 19.5 R_E) to explore all regions of the Earth's magnetosphere. The mission and its payload are described by Escoubet et al. (1997).

RAPID (Research with Adaptive Particle Imaging Detectors) (Wilken et al., 1997) is an energetic particle spectrometer, measuring the 3-D distribution of electrons (39 to 400 keV) and ions (protons 28 keV to 4 MeV, helium 137 keV to 4 MeV, oxygen 270 keV to 4 MeV).

The electrons are detected by 3 sets of 3 microstrip solid state detectors, each set being a "pin-hole camera" with a single entrance aperture, covering a total angular range of 60°. The sets, or heads, thus cover the full 180° in the half-plane containing the spin axis, with an angular resolution of 20° in the polar direction. Through the rotation of the spacecraft (period ∼4 s) the measurements can be sorted into up to 16 azimuthal sectors of 22.5°. The energy of the electrons is determined by the signal strength in the absorbing solid state detector, and is sorted into up to 8 energy channels.

The ions are measured in an independent detection system consisting of again 3 heads each covering 60°. Each head has an entrance aperture, a time-of-flight system, and a solid state detector to measure the incoming particle energy. Together, flight time and particle energy allow the ion mass and thus species to be identified. In addition, the incoming direction can be determined electronically to within 15°. Thus each ion head can be subdivided into 4 subdirections, for a total of 12 directions in the half-plane containing the spin axis. As for the electrons, the ion data can be sorted into 16 azimuthal sectors through the spinning of the spacecraft. The ion energies are sorted into up to 8 energy channels.

Because of the relatively wide energy channels, it is not immediately obvious to which energy the measured differential flux is to be assigned. The answer is in fact dependent on the steepness of the spectrum. This issue of spectral analysis with wide energy channels is treated in depth by Kronberg and Daly (2013).

The energies measured by RAPID represent the high energy tail of the full spectrum; the thermal energies are covered by the CIS experiment (Rème et al., 2001). How these datasets are combined is treated by Kronberg et al. (2010).

All the Cluster data are readily available online at the Cluster Science Archive (`https://csa.esac.esa.int/csa-web/`). An overview of the RAPID data products is given by Daly and Kronberg (2010).

3 Origin of energetic particles in the region upstream of the Earth's bow shock

3.1 Solar maximum

Interaction of the supersonic solar wind with the terrestrial magnetic field forms the bow shock. Upstream of the Earth's bow shock one can observe the generation of low frequency hydrodynamic waves, see Figure 2 on the left. Furthermore, the so-called upstream events are observed in this region. These are events during which the enhanced intensities of energetic charged particles are observed, see Figure 3 on the right. It is believed that these particles are scattered by the upstream waves leading to diffusive transport and Fermi-acceleration of the first order (Lee, 1982). It has been shown that, to be observed, stable Interplanetary Magnetic Field (IMF) conditions with direct connection to the bow shock are required, e.g., (Lin et al., 1974; Scholer et al., 1979). In Kronberg et al. (2009) we have examined whether this theory can be confirmed by observations from the Cluster mission. An analysis of the ion density gradients has shown that they fall-off exponentially with the distance from the bow shock independent on the species and charge. This means that the dynamics of ions of different species is determined by the same mechanisms. The diffusion coefficient of the ion transport is linear dependent on energy per charge in accordance with the theory from Blandford and Ostriker (1978). The mechanism leads to ion acceleration in the region upstream of the bow shock. This region crosses, for example, XMM Newton X-Ray telescope (Jansen et al., 2001). The upstream ions can affect the observations of the telescope leading to their losses (Kronberg et al., 2020). This mechanism is particularly efficient for long-living stable IMF direction and a strong shock. Such conditions are typical for Coronal Mass Ejections (CMEs). CMEs are tremendous eruptions of plasma from the Sun's upper atmosphere which mainly occur during high solar activity. The associated with CME emerging plasma bubbles have strong, relatively stable magnetic field and high propagation speed forming strong shock.

3.2 Declining phase of the solar cycle

During the declining phase of a solar cycle the terrestrial magnetosphere often encounters fast solar winds, called High Speed Streams (HSSs). The HSSs overtake regular slow solar wind and form shocks named Corotating Interaction Regions (CIRs). HSSs are coupled with Alfvén waves. The interaction between CIRs (associated with shocks and therefore enhanced solar wind dynamic pressure), the Alfvén waves in HSSs (associated with change of IMF B_z (Desai et al., 2008)) and the terrestrial magnetic field may trigger magnetospheric substorms. Substorms are associated with the magnetic field reconfiguration, charged particle acceleration and occurrence of polar aurora. Moreover, they lead to a lost of charged particles from the magnetosphere. In 2007 upstream events were discovered at a distance of up to 1750 R_E upstream of the Earth's bow shock by the mission STEREO-A (Desai et al., 2008). The origin of such events was at first unclear. We have studied 117 such events with the help of STEREO-A, STEREO-B, ACE, Geotail and Cluster satellites (Kronberg et al., 2011), see Figure 3. Thereby three theories were tested: (1) leakage of particles from the magnetosphere during substorms, e.g. (Sarris et al., 1978); (2) first order Fermi-acceleration of particles upstream of the bow shock (Lee, 1982); (3) Fermi-acceleration between Alfvén waves in CIR and the bow shock (Desai et al., 2008). It was found that more than 50% of the upstream events have magnetospheric origin. The presence of oxygen ions, energetic electrons, particle flow in the sunward direction and simultaneous occurrence of geomagnetic activity were the main characteristics to support this conclusion. This and also by Kronberg et al. (2015) studies showed that the magnetosphere loses a significant amount of plasma also at the dayside. In Savin et al. (2014) it was demonstrated that solar wind and foreshock disturbances triggered by resonant oscillations in the outer magnetospheric regions (e.g., in the bow shock surface and the magnetosheath (cavity modes)) modulate oxygen outflow from the magnetosphere into the solar wind.

4 Charged particle acceleration in the plasma sheet

Particles trapped on closed magnetospheric magnetic field lines form the plasma sheet at the nightside. This is the main reservoir of the magnetospheric plasma. In the plasma sheet the energy of ions and electrons can increase many orders of magnitude. Adiabatic mechanisms such as betatron and Fermi acceleration lead to electron energization in the plasma sheet during charge particle's drift towards the Earth. However, these acceleration mechanisms have limits. For example, Malykhin, Grigorenko, Kronberg, and Daly (2018) showed that the betatron acceleration works for electrons at energies up to 90 keV. The ions are effectively accelerated by non-adiabatic processes. Ion drift along quasi-steady dawn-dusk electric field leads to acceleration of ions up to energies of $\sim$100 keV (value of the cross-tail potential drop in the magnetotail during highly disturbed geomagnetic activity). Therefore, much effort has been put into investigations of addi-

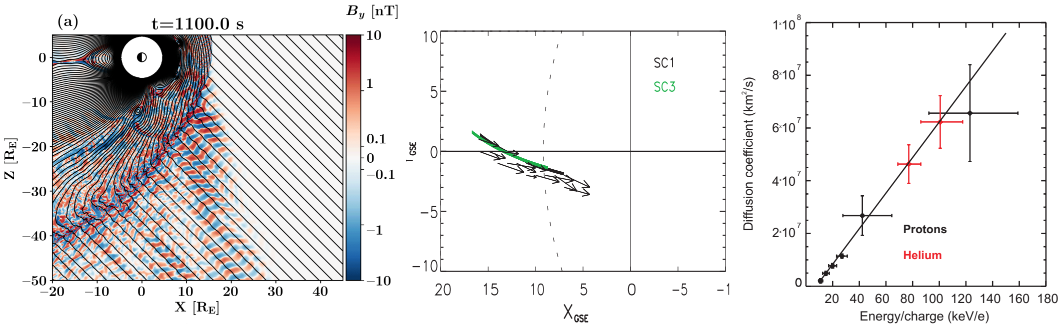

Figure 2. Left: Overview of the upstream region in a simulation with out-of-plane magnetic field fluctuations, indicating the extent of the ultra low frequency (ULF) waves in the upstream region. Black curves show magnetic field lines. Taken from Battarbee et al. (2020). Middle: Trajectories of Cluster satellites along the magnetic fields which are shown by arrows. Right: Diffusion coefficient as a function of energy per charge for protons and helium in the region upstream of the Earth's bow shock. Taken from Kronberg et al. (2009).

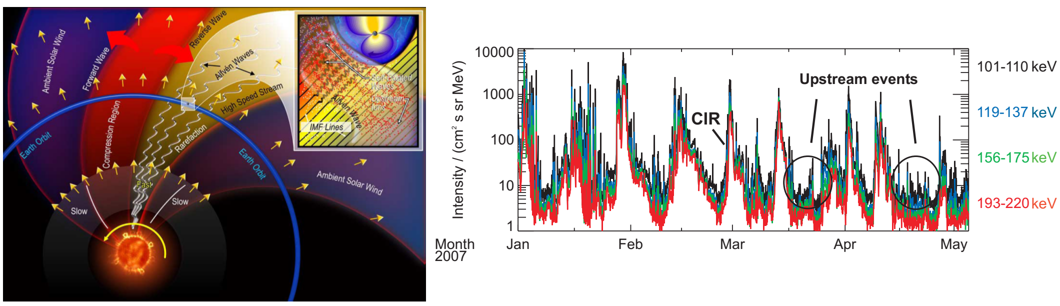

Figure 3. Left: Cartoon is showing Alfvén waves embedded within the rarefaction regions of the HSSs that follow CIRs. The rarefaction regions are associated with upstream events. Taken from Desai et al. (2008). Right: 1 h averaged proton intensity from the STEREO-A/SEPT antisunward sensor (Müller-Mellin et al., 2007) shows CIRs profiles on the scale of weeks and upstream events as small spikes on scales of hours. Taken from Kronberg et al. (2011).

tional acceleration mechanisms that can boost particle energies from ∼30 to 100s of keV range.

Many studies indicate that the energy increase is associated with the reconnection of magnetic fields and its consequences. Related mechanisms of electron acceleration were discussed, e.g., in Hoshino (2005); Birn et al. (2012). Cluster/RAPID observations demonstrated that electrons can be effectively accelerated while they are flowing into the X-line along the separatrix (Wang et al., 2013). These results imply that the electron acceleration region is significantly larger than the size of the predicted electron diffusion region in the classical Hall magnetic reconnection model. Retinò et al. (2008) showed that the presence of thin current sheets and associated electromagnetic field fluctuations are essential for the acceleration of energetic electrons during reconnection. Electromagnetic waves can transfer their energy to particles.

A consequence of magnetic field reconnection or other plasma instabilities is the dipolarization which leads to significant increase of the meridional magnetic field component on the scale of 10 minutes, see Figure 4, upper right plot. During development of the dipolarization energetic electron fluxes increase. Malykhin, Grigorenko, Kronberg, and Daly (2018) showed that this is mainly the effect of the betatron acceleration for energies up to 90 keV . Asano et al. (2010) and Malykhin, Grigorenko, Kronberg, and Daly (2018) found that there is a need for non-adiabatic acceleration mechanisms to explain electron intensities at higher energies. When the increase of the meridional magnetic field component is sudden and on scales of seconds, such an increase is called dipolarization front (Nakamura et al., 2002; Fu, Khotyaintsev, Vaivads, André, & Huang, 2012). It can be also superimposed on the dipolarization, see Figure 4, upper right plot. Fu, Khotyaintsev, Vaivads, André, Sergeev, et al. (2012); Liu et al. (2017) demonstrated that betatron and Fermi acceleration act behind the dipolarisation fronts.

Electromagnetic fluctuations in a wide frequency range play a role in particle heating and acceleration during dipolarizations. For example, high-frequency whistler waves with frequencies between proton plasma frequency and electron gyrofrequency may lead to electron heating and to a decrease in the ratio of hydrogen to electron temperature (T_p/T_e) – an important parameter for the current sheet dynamics (Grigorenko et al., 2016). In this study it was important to include energetic protons in the calculations of the temperature to avoid its underestimation.

Luo et al. (2014) using Cluster observations showed that the ion acceleration is related to the presence of X-lines near the Earth. The ion diffusion region is not known as an effective ion acceleration region (Birn et al., 2012). Therefore, consequences of reconnection such as plasmoids and magnetic field dipolarizations may lead to ion acceleration. Grigorenko et al. (2015) showed that heavy ions will be more effectively accelerated than protons when they are trapped in a plasmoid associated with certain level of electromagnetic fluctuations.

Ions interacting with dipolarizations associated with low frequency waves in the range between proton and oxygen cyclotron frequencies can be effectively accelerated (Grigorenko et al., 2017). Different particle species such as protons, helium and oxygen are accelerated by resonant interaction with electromagnetic fluctuations at the corresponding ion component gyrofrequencies. Protons are effectively accelerated by the dipolarization fronts superimposed on the dipolarization. The thickness of the fronts is less than a gyroradius of thermal protons (Runov et al., 2009; Balikhin et al., 2014) which ensures the nonadiabatic acceleration of protons, see Figure 4 (Malykhin, Grigorenko, Kronberg, Koleva, et al., 2018; Parkhomenko et al., 2018).

Malykhin et al. (2019) demonstrated that some fraction of light ions can be accelerated up to energies ≤600 keV and some fraction of oxygen ions can be accelerated up to ∼1.2 MeV during dipolarization. Such strong energy gains cannot be explained by

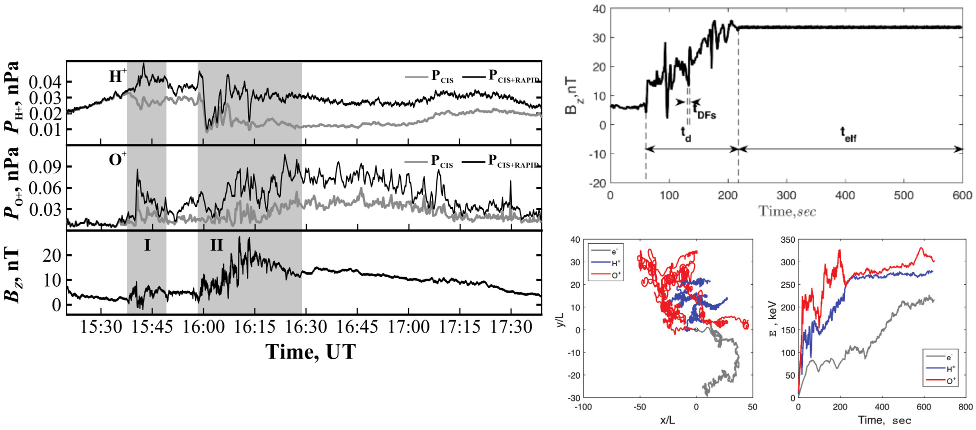

Figure 4. Left: Observation of two dipolarizations (shaded in gray) of the magnetic field in the near-Earth tail. Top to bottom: time profiles of the thermal pressure of H^+ and O^+ ions calculated based on CIS/CODIF observations (<40 keV) (shown by the gray lines) and time profiles of the pressure calculated considering the energetic component of the spectrum based on RAPID observations (shown by the black lines); time profile of the B_z magnetic field component. Adapted from Malykhin et al. (2020). Right: Trajectories and energy variation with time of electrons, protons and oxygen (bottom) during the magnetic field dipolarization associated with multiple dipolarization fronts (top) for times t_{d} and t_{elf}. Taken from Parkhomenko et al. (2018).

acceleration at a single propagating dipolarization front associated with dipolarization. A possibility of multistage ion acceleration in the course of interaction with multiple dipolarization fronts during dipolarizations (see illustration of such magnetic structures in the upper right Figure 4) is suggested to explain acceleration of ions to such high energies.

In summary, interaction of charged particles with multi-scale magnetic field structures and/or electromagnetic fluctuations which are the consequences of reconnection or other plasma instabilities, leads to effective acceleration. Multiple interaction with such structures boosts the energies even higher.

4.1 Contribution to the plasma pressure

The accelerated ions strongly affect the plasma pressure. The plasma pressure during magnetic field dipolarizations can be underestimated by a factor of >2 if the ions at energies >40 keV are neglected (Kronberg et al., 2017; Malykhin et al., 2020), see Figure 4 on the left. This is especially related to contribution of heavy energetic ionospheric ions. Nakamura et al. (2013) have shown that the pressure gradient force exceeding the Earthward directed $\vec{j}\times\vec{B}$ led to the flow bouncing during a dipolarization affecting the dynamics of the associated substorm. In this work it was essential to consider contribution to the plasma pressure of the energetic particles measured by the RAPID instrument. Influence of the energetic ions on the magnetic storm dynamics is described in Section 7.

5 Distribution on closed magnetic field lines

A considerable part of the charged particles from the solar wind and the ionosphere are trapped on closed magnetospheric magnetic field lines. We studied the dependence of the distributions of the hydrogen and oxygen ions on such closed magnetic field lines

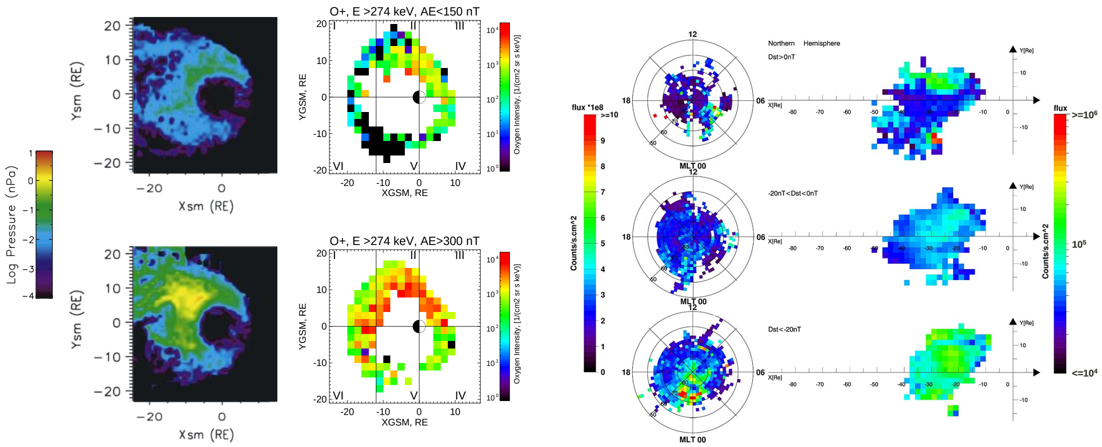

Figure 5. Left: Comparison of the oxygen pressure before the substorm and during in simulations by (Fok et al., 2006) with observations of the oxygen intensities by Cluster from Kronberg et al. (2015). Taken from Kronberg et al. (2014). Right: Map of the cold ion sources in the polar region of the Northern hemisphere and associated sinks in the plasma sheet during different geomagnetic activities. Taken from Li et al. (2013).

on the geomagnetic activity, the solar wind dynamic pressure and the direction of the IMF using 7 years of Cluster observations (Kronberg et al., 2012, 2015). The distribution of energetic ions (>274 keV) shows duskward asymmetry which is different from the rather symmetric distribution of the ions at bulk energies (∼10 keV) during geomagnetically active times (Kronberg et al., 2017). Especially strong asymmetry is seen in relation with AE-index and for oxygen ions, see Figure 5. The AE-index measures the strength of the currents in the auroral zone and indicates the strength of substorms (Nose et al., 2017). Substorms are associated with magnetic field dipolarizations and plasmoid formations which effectively accelerate charged particles as described in Section 4. An acceleration of the ions by non-adiabatic acceleration mechanisms (see Section 4 and Kronberg et al. (2015)) and gradient and curvature drifts in the duskward direction can explain duskward asymmetry. The observations agree well with the models, see, e.g., Figure 4. Another explanation of the duskward asymmetry is the distribution of cold ions with total energy <70 eV. During geomagnetically active times large amount of cold ions populate the plasma sheet closer to the Earth and more duskward than during geomagnetically quiet times due to stronger convection, see Figure 5 (Li et al., 2013). These cold ions can get effectively accelerated to many 100s of keV just within 10s of seconds, see e.g. Grigorenko et al. (2015), leading to duskward distribution of ions. This can also explain why duskward asymmetry is not observed at bulk energies for oxygen ions at distance >10 R_E during geomagnetic active times: cold ions are accelerated so fast that they do not spend much time at ∼10 keV energies.

It is remarkable that the distribution of the ions also depends on the direction of the IMF within the ecliptic plane. One can observe higher ion intensities in the regions in which reconnection between the IMF and the terrestrial magnetic field is expected. This leads to asymmetric ion distributions not only between dawn and dusk but also between the Northern and Southern hemispheres, see Figure 6. This was discovered by Luo et al. (2017) using 11 years of Cluster energetic ion (>274 keV) observations. On the dayside such asymmetry can be caused by the local acceleration in diamagnetic cavities (Nykyri et al., 2012) or entering of the particles accelerated in the upstream region of the bow shock via reconnection into the magnetosphere (Trattner et al., 2011), see Figure 6. There-

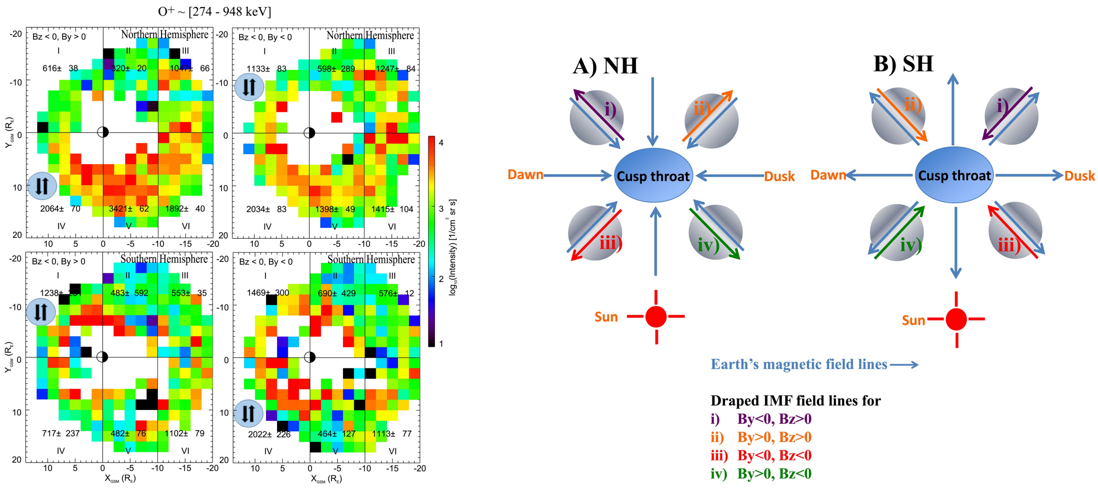

Figure 6. Left: Oxygen intensities with energy from 274 to 962 keV under southward IMF with different IMF By directions in both the Northern and Southern Hemispheres. The gray circles with antiparallel arrows indicate quadrants where the reconnection and location of diamagnetic cavity is expected. Right: Arrows indicate the Earth's magnetic field and the draped IMFs for each orientation. Shaded gray regions show under each IMF orientation where the most antiparallel components are located relative to the cusp region and where the diamagnetic cavity can form and trap the particles. Taken from Luo et al. (2017).

fore, not only substorm related acceleration processes lead to asymmetries on the closed magnetic field lines.

6 Substorm dynamics

Energetic particles help to reveal different aspects related to substorm dynamics, for example causes of associated dispersionless injections of electrons at geostationary orbits. A classic substorm event with several dispersionless injections was investigated using data from 15 satellites by Kronberg et al. (2017). These were data from 4 Cluster satellites, 3 THEMIS satellites, 6 LANL satellites and 2 Van Allen Probes. These data were expanded by the magnetic field observations measured by many stations at high latitudes from INTERMAGNET (St-Louis, 2008) and SuperMAG (Gjerloev, 2012) networks. Such injections feed with charged particles the ring current and the radiation belts, the most important regions for the space weather effects. The origin of dispersionless injections is controversial. In this study it was shown that during different phases of the substorm event the reasons for the injections can be different: dynamic motion of plasma sheet structures during the growth phase, current wedge formation during the substorm onset and magnetic dipolarization fronts during the expansion phase. Only the injection associated with the substorm onset and formation of the current wedge filled the radiation belts and ring current with a substantial number of charged particles.

Another important result of this study is that the currents along the magnetic fields formed as a result of the substorm and related to the magnetosphere-ionosphere coupling, can be responsible for the electron acceleration at geostationary orbits. The acceleration leads to the formation of a so-called bump on the tail of the electron intensity spectra at the geosynchronous orbit but not in the tail region observed by Cluster. It is suggested that this effect occurs because of drift-resonant interaction with ULF waves generated by the field-aligned currents.

7 Magnetic storms

The accelerated particles move in the direction of the Earth and then drift around, forming the ring current. The ring current generates a magnetic field in the southward direction at the Earth's surface, namely a field in the opposite direction to the terrestrial magnetic field, produced by the Earth's dynamo. The terrestrial magnetic field will be reduced and this disturbance is called magnetic storm, one of the most important characteristics of the space weather. The influence of the ionospheric and energetic particles on the strength of the magnetic storm was investigated in Kronberg et al. (2017). Both of these components are often neglected in the calculation of the plasma pressure as in the plasma sheet as well in the ring current. Haaland et al. (2010) showed that the power law part of the proton spectra (energetic part) becomes significantly harder in the plasma sheet during magnetic storms. Our calculations demonstrated that the plasma pressure and as a consequence the Dst-index (represents the strength of the magnetic storm near the equator (Nose et al., 2017)) are strongly underestimated when the ionospheric ions and ions at energies > 40 keV are neglected. The Space Weather Modeling Frame (Tóth et al., 2012) simulations with two different ionospheric ion outflow models as an input have shown similar to observations results. The space weather modeling, however, still can be improved by considering energetic part of the particle spectra.

8 Radiation belts

The Van Allen radiation belts are a region with highly-energetic (>100 keV) charged particles, mainly electrons and protons, trapped by the terrestrial magnetic field. The radiation belts are hazardous for satellite operation. The electrons with energies of tens of keV, injected into the inner magnetosphere as a result of substorm activity, produce waves, and can be accelerated to higher energies. The particles with energies of hundreds of keV can accumulate at the surface of the spacecraft, leading to surface-charging effects, and can penetrate deep into instrument electronics causing satellite anomalies and instrument malfunctions by deep dielectric charging, e.g. (Baker et al., 1994, 2004).

Due to their importance for satellite operation, a large number of instruments have provided observations of the radiation belt populations. One of the longest continuous data sets of electron flux at energies 40 to 400 keV has been supplied by the RAPID/IES detector. The IES instrument was not specifically designed for radiation belt studies, and therefore is subject to background contamination by higher energy electrons and protons. The effect of the charged particle radiation belt environment on the RAPID/IES detector was investigated in Kronberg et al. (2016). For this the IES detector was simulated in the Geant4 environment (Agostinelli et al., 2003). The percentages of the total electron intensity attributed to contamination were calculated for L-shells up to 9. The background-corrected measurements were compared to the observations by the MagEIS detector aboard the Van Allen Probes mission (Blake et al., 2013) during October-December 2012, and the ratio between the two data sets was close to 1.

Smirnov et al. (2019) compared the background-corrected electron flux measurements by the IES detector to those by RBSP/MagEIS in 2012-2016, both in terms of omnidirectional flux and flux at 90° pitch angle. It was found that the corrected Cluster measurements were close to the MagEIS observations during the 2012-2016 period. These background-corrected observations can be used in various scientific applications. Breuillard et al. (2015) derived energetic electron anisotropy to model the chorus wave power distribution in the outer radiation belt. Smirnov et al. (2019) presented a long-term analysis of electron flux dynamics during ~ 1.5 solar cycles in 2001-2016. It was found that the long-term trend of electron intensities at energies 40 to 400 keV in the outer belt exhibited a high positive correlation with the solar wind dynamic pressure and AE index (see Figure 7). A simple generalized empirical model which connects electron intensi-

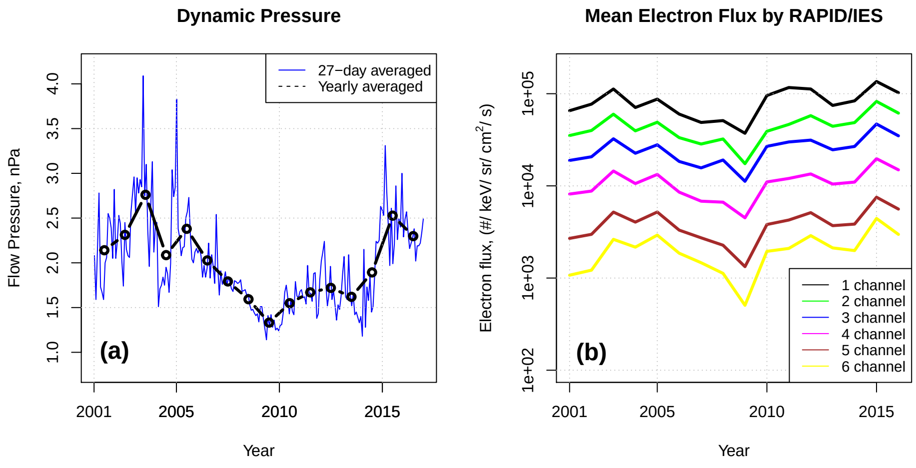

Figure 7. (a) The solar wind dynamic pressure, and (b) yearly averaged electron flux intensities by RAPID/IES. Adapted from Smirnov et al. (2019).

ties at L-shells from 4 to 6 to the solar wind dynamic pressure was derived:

$$\log_{10} y = 0.35(\pm 0.1) + 0.5(\pm 0.18)x, \tag{1}$$

where x stands for the normalized solar wind dynamic pressure and y represents the logarithm of electron flux, normalized to their minimum and maximum values.

Trapped energetic particles in planetary magnetospheres undergo three types of periodic motion, namely the gyro-, bounce, and drift motion. Each type is associated with the corresponding adiabatic invariant (μ, K, and $L^\star$, respectively), which are conserved when the magnetic field changes are slow compared to the motion periods. Electron flux, measured as a function of energy, position, and time, can be converted to phase space density (PSD), as a function of three adiabatic invariants. Analyzing the PSD behavior under the fixed values of μ, K, and $L^\star$, allows for a separation between adiabatic and non-adiabatic processes, and helps to utilize observations from different magnetic latitudes. This is of particular interest for the Cluster constellation, due to its polar orbit. The method to calculate the adiabatic invariants and convert the RAPID/IES electron flux to PSD was developed in Smirnov et al. (2020). Figure 8 shows the long-term behavior of low-μ electrons along approximately 1.5 solar cycles and the 27-day averaged F10.7 and AE indices. F10.7 index (Tapping, 2013) follows the sunspot cycle evolution, while the AE index intensifies with higher occurrence of coronal holes and HSSs during the declining phase. At L-values from 4 to 6, the general PSD behavior closely resembles the variation of the AE index. The PSD values are higher during the declining phase of the solar cycle 23 (2004–2007), and exhibit minimum values during the solar minimum in 2009, also referred to as the "radiation belts desert". RAPID/IES mainly samples low-μ electrons, for which the substorm activity is of paramount importance. These results agree well with previous findings by Zhao et al. (2017) that observed a high correlation of PSD enhancements with auroral geomagnetic indices, suggesting a direct transport of electrons from substorm injections.

9 Summary

The observations of energetic charged particles by the Cluster/RAPID instrument substantially enhanced our understanding of dynamics of the terrestrial magnetosphere. The following results were obtained:

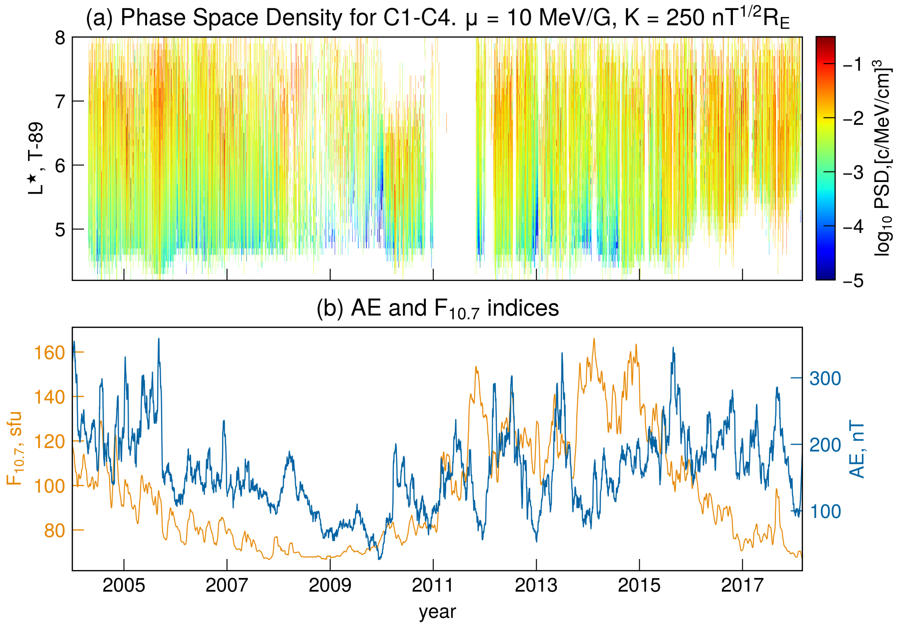

Figure 8. (a) PSD for Cluster-1 to Cluster-4 under the fixed values of adiabatic invariants in 2004-2019; (b) AE and F10.7 indices. Adapted from Smirnov et al. (2020)

Charged particle energization mechanisms were thoroughly investigated. The results demonstrate that interaction of charged particles with multi-scale magnetic field structures and/or electromagnetic fluctuations which are the consequences of reconnection or other plasma instabilities leads to an effective acceleration. Multiple interaction with such magnetic structures increases energy even higher.

The energetic particles affect the plasma temperature and pressure. The Cluster results demonstrated that the energetic part >40 keV has to be considered during geomagnetically disturbed times in the calculations of the ion plasma temperature and pressure. Otherwise, the related physics, e.g., in flow breaking region or in the ring current is incorrectly interpreted. Therefore, it is recommended to include the energetic part and ionospheric heavy ions when estimating these parameters.

The distribution of the energetic ions on the closed magnetic field lines is strongly affected by the solar wind and geomagnetic activity. A substantial amount of ions escape the magnetosphere populating the region upstream of the bow shock. Surprisingly the distribution is also affected by the IMF B_y direction leading to dawn-dusk asymmetries as well as to asymmetries between Northern and Southern hemispheres. This also implies the importance of reconnection processes effects on the energetic ion distribution not only at the night side but also at the dayside of the magnetosphere.

The radiation belts are effectively filled with electrons during substorms onsets. Clear relation of electron intensities in the radiation belts at L-shells 4 to 6 and substorm activity was demonstrated for approximately 1.5 solar cycles.

A large data set of electron intensities in the radiation belts and ring current region is available for scientific investigations, thanks to the recently developed background-correction technique. The Cluster constellation is one of the longest ongoing missions in the Earth's magnetosphere, providing more than 20 years of observations. The IES detector, similar to that on Cluster, was carried by the Polar mission and is also included in the payload of the recently launched BeiDou GNSS constellation. The combined data set thus covers more than 2 solar cycles. It can be useful for the long-term statistical analysis of electron flux behavior in the outer radiation belt, and can be incorporated into the empirical models of the medium energy electron flux, e.g, by Smirnov et al. (2020). Moreover, the electron fluxes converted to PSD can be used to set up boundary conditions for radiation belts modeling, as well as for data assimilation purposes.

The vast amount of RAPID data collected within the last 20 years, available at the Cluster Science Archive, is welcoming future explorations.

Acknowledgments

EK is supported by German Research Foundation (DFG) under number KR 4375/2-1 within SPP "Dynamic Earth". AGS was supported by the DFG for SFB 1294, project No. 318763901. The work of EK, EG and AM is supported by the Volkswagen Foundation grant Az. 97 742. PWD acknowledges DLR grant 50 OC 1602. Data were not used, nor created for this research.

References

Aellig, M. R., Lazarus, A. J., & Steinberg, J. T. (2001, January). The solar wind helium abundance: Variation with wind speed and the solar cycle. *Geophys. Res. Lett.*, *28*(14), 2767-2770. doi: 10.1029/2000GL012771

Agostinelli, S., Allison, J., Amako, K., Apostolakis, J., Araujo, H., Arce, P., ... Zschiesche, D. (2003). Geant4 a simulation toolkit. *Nuclear Instruments and Methods in Physics Research Section A: Accelerators, Spectrometers, Detectors and Associated Equipment*, *506*(3), 250 - 303. doi: http://dx.doi.org/10.1016/S0168-9002(03)01368-8

Asano, Y., Shinohara, I., Retinò, A., Daly, P. W., Kronberg, E. A., Takada, T., ... Rème, H. (2010, May). Electron acceleration signatures in the magnetotail associated with substorms. *Journal of Geophysical Research (Space Physics)*, *115*(A5), A05215. doi: 10.1029/2009JA014587

Baker, D. N., Kanekal, S., Blake, J. B., Klecker, B., & Rostoker, G. (1994, January). Satellite anomalies linked to electron increase in the magnetosphere. *EOS Transactions*, *75*(35), 401-405. doi: 10.1029/94EO01038

Baker, D. N., Kanekal, S. G., & Blake, J. B. (2004, February). Characterizing the Earth's outer Van Allen zone using a radiation belt content index. *Space Weather*, *2*(2), S02003. doi: 10.1029/2003SW000026

Balikhin, M. A., Runov, A., Walker, S. N., Gedalin, M., Dandouras, I., Hobara, Y., & Fazakerley, A. (2014, August). On the fine structure of dipolarization fronts. *Journal of Geophysical Research (Space Physics)*, *119*(8), 6367-6385. doi: 10.1002/2014JA019908

Battarbee, M., Blanco-Cano, X., Turc, L., Kajdič, P., Johlander, A., Tarvus, V., ... Palmroth, M. (2020). Helium in the earth's foreshock: a global vlasiator survey. *Annales Geophysicae*, *38*(5), 1081–1099. doi: 10.5194/angeo-38-1081-2020

Birn, J., Artemyev, A. V., Baker, D. N., Echim, M., Hoshino, M., & Zelenyi, L. M. (2012, November). Particle Acceleration in the Magnetotail and Aurora. *Space Sci. Rev.*, *173*, 49-102. doi: 10.1007/s11214-012-9874-4

Blake, J. B., Carranza, P. A., Claudepierre, S. G., Clemmons, J. H., Crain, W. R., Dotan, Y., ... Zakrzewski, M. P. (2013, November). The Magnetic Electron Ion Spectrometer (MagEIS) Instruments Aboard the Radiation Belt Storm Probes (RBSP) Spacecraft. *Space Sci. Rev.*, *179*, 383-421. doi: 10.1007/s11214-013-9991-8

Blandford, R. D., & Ostriker, J. P. (1978, April). Particle acceleration by astrophysical shocks. *Astrophysical Journal*, *221*. doi: 10.1086/182658

Borovsky, J. E., Delzanno, G. L., Valdivia, J. A., Moya, P. S., Stepanova, M., Birn, J., ... Hesse, M. (2020, October). Outstanding questions in magnetospheric plasma physics: The pollenzo view. *Journal of Atmospheric and Solar-Terrestrial Physics*, *208*, 105377. doi: 10.1016/j.jastp.2020.105377

Borrini, G., Gosling, J. T., Bame, S. J., & Feldman, W. C. (1982, September). Helium abundance enhancements in the solar wind. *J. Geophys. Res.*, *87*(A9), 7370-7378. doi: 10.1029/JA087iA09p07370

Breuillard, H., Agapitov, O., Artemyev, A., Kronberg, E. A., Haaland, S. E., Daly, P. W., ... Rolland, G. (2015). Field-aligned chorus wave spectral power in Earth's outer radiation belt. *Annales Geophysicae*, *33*, 583-597. doi: 10.5194/angeo-33-583-2015

Daly, P. W., & Kronberg, E. A. (2010). RAPID Products at the Cluster Active Archive. In Laakso, H., Taylor, M., & Escoubet, C. P. (Ed.), *The cluster active archive, studying the earth's space plasma environment* (p. 145-158). doi: 10.1007/978-90-481-3499-1_9

Desai, M. I., Mason, G. M., Müller-Mellin, R., Korth, A., Mall, U., Dwyer, J. R., & von Rosenvinge, T. T. (2008, August). The spatial distribution of upstream ion events from the Earth's bow shock measured by ACE, Wind, and STEREO. *J. Geophys. Res.*, *113*, 8103. doi: 10.1029/2007JA012909

Escoubet, C. P., Schmidt, R., & Goldstein, M. L. (1997, January). Cluster - Science and Mission Overview. *Space Science Reviews*, *79*, 11-32.

Fioretti, V., Bulgarelli, A., Malaguti, G., Spiga, D., & Tiengo, A. (2016). Monte Carlo simulations of soft proton flares: testing the physics with XMM-Newton. In *Society of photo-optical instrumentation engineers (spie) conference series* (Vol. 9905, p. 99056W). doi: 10.1117/12.2232537

Fok, M., Moore, T. E., Brandt, P. C., Delcourt, D. C., Slinker, S. P., & Fedder, J. A. (2006, October). Impulsive enhancements of oxygen ions during substorms. *J. Geophys. Res.*, *111*, 10222. doi: 10.1029/2006JA011839

Fu, H. S., Khotyaintsev, Y. V., Vaivads, A., André, M., & Huang, S. Y. (2012, May). Occurrence rate of earthward-propagating dipolarization fronts. *Geophys. Res. Lett.*, *39*(10). doi: 10.1029/2012GL051784

Fu, H. S., Khotyaintsev, Y. V., Vaivads, A., André, M., Sergeev, V. A., Huang, S. Y., ... Daly, P. W. (2012, December). Pitch angle distribution of suprathermal electrons behind dipolarization fronts: A statistical overview. *Journal of Geophysical Research (Space Physics)*, *117*(A12), A12221. doi: 10.1029/2012JA018141

Gjerloev, J. W. (2012, September). The SuperMAG data processing technique. *Journal of Geophysical Research (Space Physics)*, *117*, A09213. doi: 10.1029/2012JA017683

Gloeckler, G., & Geiss, J. (1989). The abundances of elements and isotopes in the solar wind. *AIP Conference Proceedings*, *183*(1), 49-71. doi: 10.1063/1.37985

Grigorenko, E. E., Kronberg, E. A., & Daly, P. W. (2017, January). Heating and acceleration of charged particles during magnetic dipolarizations. *Cosmic Research*, *55*, 57-66. doi: 10.1134/S0010952517010063

Grigorenko, E. E., Kronberg, E. A., Daly, P. W., Ganushkina, N. Y., Lavraud, B., Sauvaud, J.-A., & Zelenyi, L. M. (2016, October). Origin of low proton-to-electron temperature ratio in the Earth's plasma sheet. *J. Geophys. Res.*, *121*, 9985-10. doi: 10.1002/2016JA022874

Grigorenko, E. E., Malykhin, A. Y., Kronberg, E. A., Malova, K. V., & Daly, P. W. (2015, August). Acceleration of ions to suprathermal energies by turbulence in the plasmoid-like magnetic structures. *J. Geophys. Res.*, *120*, 6541-6558. doi: 10.1002/2015JA021314

Haaland, S., Kronberg, E. A., Daly, P. W., Fränz, M., Degener, L., Georgescu, E., & Dandouras, I. (2010, August). Spectral characteristics of protons in the Earth's plasmasheet: statistical results from Cluster CIS and RAPID. *Ann. Geophys.*, *28*, 1483-1498. doi: 10.5194/angeo-28-1483-2010

Hoshino, M. (2005, October). Electron surfing acceleration in magnetic reconnection. *Journal of Geophysical Research (Space Physics)*, *110*(A10), A10215. doi: 10.1029/2005JA011229
Jansen, F., Lumb, D., Altieri, B., Clavel, J., Ehle, M., Erd, C., ... Vacanti, G. (2001, January). XMM-Newton observatory. I. The spacecraft and operations. *Astronomy and Astrophysics*, *365*, L1-L6. doi: 10.1051/0004-6361:20000036
Kasper, J. C., Stevens, M. L., Lazarus, A. J., Steinberg, J. T., & Ogilvie, K. W. (2007, May). Solar Wind Helium Abundance as a Function of Speed and Heliographic Latitude: Variation through a Solar Cycle. *Astropys. J.*, *660*(1), 901-910. doi: 10.1086/510842
Kronberg, E. A., Ashour-Abdalla, M., Dandouras, I., Delcourt, D. C., Grigorenko, E. E., Kistler, L. M., ... Zelenyi, L. M. (2014, November). Circulation of Heavy Ions and Their Dynamical Effects in the Magnetosphere: Recent Observations and Models. *Space Sci. Rev.*, *184*, 173-235. doi: 10.1007/s11214-014-0104-0
Kronberg, E. A., Bučík, R., Haaland, S., Klecker, B., Keika, K., Desai, M. I., ... Lui, A. T. Y. (2011, February). On the origin of the energetic ion events measured upstream of the Earth's bow shock by STEREO, Cluster, and Geotail. *J. Geophys. Res.*, *116*, 2210. doi: 10.1029/2010JA015561
Kronberg, E. A., & Daly, P. W. (2013, August). Spectral analysis for wide energy channels. *Geoscientific Instrumentation, Methods and Data Systems Discussions*, *3*, 533-546. doi: 10.5194/gid-3-533-2013
Kronberg, E. A., Daly, P. W., Dandouras, I., Haaland, S., & Georgescu, E. (2010). Generation and Validation of Ion Energy Spectra Based on Cluster RAPID and CIS Measurements. In Laakso, H., Taylor, M., & Escoubet, C. P. (Ed.), *The cluster active archive, studying the earth's space plasma environment* (p. 301-306). doi: 10.1007/978-90-481-3499-1_20
Kronberg, E. A., Gastaldello, F., Haaland, S., Smirnov, A., Berrendorf, M., Ghizzardi, S., ... Kistler, L. (2020, November). Prediction and Understanding of Soft-proton Contamination in XMM-Newton: A Machine Learning Approach. *Astrophys. J.*, *903*(2), 89. doi: 10.3847/1538-4357/abbb8f
Kronberg, E. A., Grigorenko, E. E., Haaland, S. E., Daly, P. W., Delcourt, D. C., Luo, H., ... Dandouras, I. (2015, May). Distribution of energetic oxygen and hydrogen in the near-Earth plasma sheet. *J. Geophys. Res.*, *120*, 3415-3431. doi: 10.1002/2014JA020882
Kronberg, E. A., Grigorenko, E. E., Turner, D. L., Daly, P. W., Khotyaintsev, Y., & Kozak, L. (2017, March). Comparing and contrasting dispersionless injections at geosynchronous orbit during a substorm event. *J. Geophys. Res.*, *122*, 3055-3072. doi: 10.1002/2016JA023551
Kronberg, E. A., Haaland, S. E., Daly, P. W., Grigorenko, E. E., Kistler, L. M., Fränz, M., & Dandouras, I. (2012, December). Oxygen and hydrogen ion abundance in the near-Earth magnetosphere: Statistical results on the response to the geomagnetic and solar wind activity conditions. *J. Geophys. Res.*, *117*, 12208. doi: 10.1029/2012JA018071
Kronberg, E. A., Kis, A., Klecker, B., Daly, P. W., & Lucek, E. A. (2009, March). Multipoint observations of ions in the 30-160 keV energy range upstream of the Earth's bow shock. *J. Geophys. Res.*, *114*, 3211. doi: 10.1029/2008JA013754
Kronberg, E. A., Li, K., Grigorenko, E. E., Maggiolo, R., Haaland, S., Daly, P. W., & Luo, H. (2017). Dawn-Dusk Asymmetries in the Near-Earth Plasma Sheet: Ion Observations [Article; Book Chapter]. In Haaland, S and Runov, A and Forsyth, C (Ed.), *Dawn-dusk asymmetries in planetary plasma environments* (Vol. 230, p. 243-253). 2000 Florida Ave NW, Washington, DC 20009 USA: American Geophysical Union.
Kronberg, E. A., Rashev, M. V., Daly, P. W., Shprits, Y. Y., Turner, D. L., Droz-

dov, A., … Friedel, R. (2016, June). Contamination in electron observations of the silicon detector on board Cluster/RAPID/IES instrument in Earth's radiation belts and ring current. *Space Weather*, *14*, 449-462. doi: 10.1002/2016SW001369

Kronberg, E. A., Welling, D., Kistler, L. M., Mouikis, C., Daly, P. W., Grigorenko, E. E., … Dandouras, I. (2017, September). Contribution of energetic and heavy ions to the plasma pressure: The 27 September to 3 October 2002 storm. *J. Geophys. Res.*, *122*, 9427-9439. doi: 10.1002/2017JA024215

Lee, M. A. (1982, July). Coupled hydromagnetic wave excitation and ion acceleration upstream of the earth's bow shock. *J. Geophys. Res.*, *87*, 5063-5080.

Li, K., Haaland, S., Eriksson, A., André, M., Engwall, E., Wei, Y., … Ren, Q. Y. (2013, September). Transport of cold ions from the polar ionosphere to the plasma sheet. *J. Geophys. Res.*, *118*, 5467-5477. doi: 10.1002/jgra.50518

Lin, R. P., Meng, C.-I., & Anderson, K. A. (1974, February). 30- to 100-keV protons upstream from the Earth's bow shock. *J. Geophys. Res.*, *79*, 489-498.

Liu, C. M., Fu, H. S., Cao, J. B., Xu, Y., Yu, Y. Q., Kronberg, E. A., & Daly, P. W. (2017, October). Rapid Pitch Angle Evolution of Suprathermal Electrons Behind Dipolarization Fronts. *Geophys. Res. Lett.*, *44*(20), 10,116-10,124. doi: 10.1002/2017GL075007

Luo, H., Kronberg, E. A., Grigorenko, E. E., Fränz, M., Daly, P. W., Chen, G. X., … Wei, Y. (2014, June). Evidence of strong energetic ion acceleration in the near-Earth magnetotail. *Geophys. Res. Lett.*, *41*, 3724-3730. doi: 10.1002/2014GL060252

Luo, H., Kronberg, E. A., Nykyri, K., Trattner, K. J., Daly, P. W., Chen, G. X., … Ge, Y. S. (2017, May). IMF dependence of energetic oxygen and hydrogen ion distributions in the near-Earth magnetosphere. *J. Geophys. Res.*, *122*, 5168-5180. doi: 10.1002/2016JA023471

Müller-Mellin, R., Böttcher, S., Falenski, J., Rode, E., Duvet, L., Sanderson, T. R., … Smit, H. (2007). The Solar Electron and Proton Telescope for the STEREO mission. *Space Sci. Rev.*. doi: 10.1007/s11214-007-9204-4a

Malykhin, A. Y., Grigorenko, E. E., Kronberg, E. A., & Daly, P. (2020, April). Variations in Ion-Component Pressure during Dipolarization in the Near-Earth Magnetotail Plasma Sheet. *Geomagnetism and Aeronomy*, *60*(1), 20-27. doi: 10.1134/S0016793220010090

Malykhin, A. Y., Grigorenko, E. E., Kronberg, E. A., & Daly, P. W. (2018, December). The Effect of the Betatron Mechanism on the Dynamics of Superthermal Electron Fluxes within Dipolizations in the Magnetotail. *Geomagnetism and Aeronomy*, *58*(6), 744-752. doi: 10.1134/S0016793218060099

Malykhin, A. Y., Grigorenko, E. E., Kronberg, E. A., Daly, P. W., & Kozak, L. V. (2019, July). Acceleration of protons and heavy ions to suprathermal energies during dipolarizations in the near-Earth magnetotail. *Annales Geophysicae*, *37*(4), 549-559. doi: 10.5194/angeo-37-549-2019

Malykhin, A. Y., Grigorenko, E. E., Kronberg, E. A., Koleva, R., Ganushkina, N. Y., Kozak, L., & Daly, P. W. (2018, May). Contrasting dynamics of electrons and protons in the near-Earth plasma sheet during dipolarization. *Annales Geophysicae*, *36*, 741-760. doi: 10.5194/angeo-36-741-2018

Matéo-Vélez, J. C., Sicard, A., Payan, D., Ganushkina, N., Meredith, N. P., & Sillanpäa, I. (2018, January). Spacecraft surface charging induced by severe environments at geosynchronous orbit. *Space Weather*, *16*(1), 89-106. doi: 10.1002/2017SW001689

McComas, D. J., Alexander, N., Angold, N., Bale, S., Beebe, C., Birdwell, B., … Wilson, P. (2016, December). Integrated Science Investigation of the Sun (ISIS): Design of the Energetic Particle Investigation. *Space Science Reviews*, *204*(1-4), 187-256. doi: 10.1007/s11214-014-0059-1

Nakamura, R., Baumjohann, W., Klecker, B., Bogdanova, Y., Balogh, A., Rème, H.,

… Runov, A. (2002, October). Motion of the dipolarization front during a flow burst event observed by Cluster. *Geophys. Res. Lett.*, *29*(20), 1942. doi: 10.1029/2002GL015763

Nakamura, R., Baumjohann, W., Panov, E., Volwerk, M., Birn, J., Artemyev, A., … Khotyaintsev, Y. (2013, May). Flow bouncing and electron injection observed by Cluster. *Journal of Geophysical Research (Space Physics)*, *118*(5), 2055-2072. doi: 10.1002/jgra.50134

Neugebauer, M. (1981, May). Observations of Solar-Wind Helium. *Fundamentals of Cosmic Physics*, *7*, 131-199.

Nose, M., Sugiura, M., Kamei, T., & Iyemori, T. (2017). *Ae index.* WDC for Geomagnetism, Kyoto. doi: 10.17593/15031-54800

Nykyri, K., Otto, A., Adamson, E., Kronberg, E., & Daly, P. (2012, October). On the origin of high-energy particles in the cusp diamagnetic cavity. *Journal of Atmospheric and Solar-Terrestrial Physics*, *87*, 70-81. doi: 10.1016/j.jastp.2011.08.012

Parkhomenko, E. I., Malova, H. V., Grigorenko, E. E., Popov, V. Y., Petrukovich, A. A., Delcourt, D. C., … Zelenyi, L. M. (2018, January). Plasma Acceleration on Multiscale Temporal Variations of Electric and Magnetic Fields during Substorm Dipolarization in the Earth'S Magnetotail. *Annals of Geophysics*, *61*(3), 334. doi: 10.4401/ag-7582

Rème, H., Aoustin, C., Bosqued, J. M., Dandouras, I., Lavraud, B., Sauvaud, J. A., … Sonnerup, B. (2001, October). First multispacecraft ion measurements in and near the Earth's magnetosphere with the identical Cluster ion spectrometry (CIS) experiment. *Ann. Geophys.*, *19*, 1303-1354.

Retinò, A., Nakamura, R., Vaivads, A., Khotyaintsev, Y., Hayakawa, T., Tanaka, K., … Cornilleau-Wehrlin, N. (2008, December). Cluster observations of energetic electrons and electromagnetic fields within a reconnecting thin current sheet in the Earth's magnetotail. *J. Geophys. Res.*, *113*, 12215-+. doi: 10.1029/2008JA013511

Runov, A., Angelopoulos, V., Sitnov, M. I., Sergeev, V. A., Bonnell, J., McFadden, J. P., … Auster, U. (2009, July). THEMIS observations of an earthward-propagating dipolarization front. *Geophys. Res. Lett.*, *36*, A014106. doi: 10.1029/2009GL038980

Sarris, E. T., Krimigis, S. M., Bostrom, C. O., & Armstrong, T. P. (1978, September). Simultaneous multispacecraft observations of energetic proton bursts inside and outside the magnetosphere. *J. Geophys. Res.*, *83*, 4289-4305.

Savin, S., Amata, E., Budaev, V., Zelenyi, L., Kronberg, E. A., Buechner, J., … Lezhen, L. (2014, March). On nonlinear cascades and resonances in the outer magnetosphere. *Soviet Journal of Experimental and Theoretical Physics Letters*, *99*(1), 16-21. doi: 10.1134/S002136401401010X

Scholer, M., Gloeckler, G., Ipavich, F. M., Hovestadt, D., & Klecker, B. (1979, September). Pitch angle distributions of energetic protons near the earth's bow shock. *Geophys. Res. Lett.*, *6*, 707-710.

Smirnov, A. G., Berrendorf, M., Shprits, Y., Kronberg, E. A., Allison, H. J., Aseev, N. A., … others (2020). Medium energy electron flux in earth's outer radiation belt (MERLIN): A machine learning model. *Space Weather*, *18*(11), e2020SW002532.

Smirnov, A. G., Kronberg, E. A., Daly, P. W., Aseev, N. A., Shprits, Y. Y., & Kellerman, A. C. (2020, February). Adiabatic Invariants Calculations for Cluster Mission: A Long-Term Product for Radiation Belts Studies. *Journal of Geophysical Research (Space Physics)*, *125*(2), e27576. doi: 10.1029/2019JA027576

Smirnov, A. G., Kronberg, E. A., Latallerie, F., Daly, P. W., Aseev, N., Shprits, Y. Y., … Taylor, M. G. G. T. (2019, April). Electron Intensity Measurements by the Cluster/RAPID/IES Instrument in Earth's Radiation Belts and Ring

Current. *Space Weather*, *17*(4), 553-566. doi: 10.1029/2018SW001989

St-Louis, B. (2008). *INTERMAGNET Technical Reference Manual Version 4.4* (Tech. Rep.). INTERMAGNET internal publication, Edinburgh.

Tapping, K. F. (2013, July). The 10.7 cm solar radio flux ($F_{10.7}$). *Space Weather*, *11*(7), 394-406. doi: 10.1002/swe.20064

Tóth, G., van der Holst, B., Sokolov, I. V., De Zeeuw, D. L., Gombosi, T. I., Fang, F., ... Opher, M. (2012, February). Adaptive numerical algorithms in space weather modeling. *Journal of Computational Physics*, *231*, 870-903. doi: 10.1016/j.jcp.2011.02.006

Trattner, K. J., Petrinec, S. M., Fuselier, S. A., Nykyri, K., & Kronberg, E. (2011, September). Cluster observations of bow shock energetic ion transport through the magnetosheath into the cusp. *Journal of Geophysical Research (Space Physics)*, *116*(A9), A09207. doi: 10.1029/2011JA016617

Wang, R., Du, A., Nakamura, R., Lu, Q., Khotyaintsev, Y. V., Volwerk, M., ... Fazakerley, A. N. (2013, June). Observation of multiple sub-cavities adjacent to single separatrix. *Geophys. Res. Lett.*, *40*(11), 2511-2517. doi: 10.1002/grl.50537

Wilken, B., Axford, W. I., Daglis, I., Daly, P., Guttler, W., Ip, W. H., ... Ullaland, S. (1997, January). RAPID - The imaging energetic particle spectrometer on Cluster. *Space Sci. Rev.*, *79*, 399-473. doi: 10.1023/A:1004994202296

Yau, A. W., Whalen, B. A., & Sagawa, E. (1991, February). Minor ion composition in the polar ionosphere. *Geophys. Res. Lett.*, *18*(2), 345-348. doi: 10.1029/91GL00034

Zhao, H., Baker, D., Jaynes, A., Li, X., Elkington, S., Kanekal, S., ... Forsyth, C. (2017). On the relation between radiation belt electrons and solar wind parameters/geomagnetic indices: Dependence on the first adiabatic invariant and l. *Journal of Geophysical Research: Space Physics*, *122*(2), 1624–1642.